Molecular Pharmacology Fast Forward. Published on September 27, 2005 as doi:10.1124/mol.105.015164

MOL 15164

Determinants of zinc potentiation on the α4 subunit of neuronal nicotinic receptors

Bernard Hsiao[1], Karla B. Mihalak[1], Sarah E. Repicky, Drew Everhart,
Ana H. Mederos, Arun Malhotra and Charles W. Luetje

Department of Molecular and Cellular Pharmacology (B.H., K.B.M., S.E.R., D.E., A.H.M. and C.W.L.),
Department of Biochemistry and Molecular Biology (A.M.),
Miller School of Medicine, University of Miami, Miami, Florida 33101

Molecular Pharmacology Fast Forward. Published on September 27, 2005 as DOI: 10.1124/mol.105.015164
This article has not been copyedited and formatted. The final version may differ from this version.

Running Title: Zinc potentiation sites on neuronal nicotinic receptors

Corresponding Author: Charles W. Luetje, Ph.D.
Molecular and Cellular Pharmacology, R-189
University of Miami
P.O. Box 016189
Miami, FL 33101
305-243-4458
Fax: 305-243-4555
cluetje@chroma.med.miami.edu

33 text pages
2 Tables
6 Figures
40 References

229 words in Abstract
489 words in Introduction
1478 words in Discussion

Nonstandard Abbreviations: AChBP, acetylcholine binding protein; MTS, methanethiosulfonate; MTSEA, N-biotinoylaminoethyl methanethiosulfonate; MTSET, [2-(trimethylammonium)ethyl] methanethiosulfonate; nAChR, nicotinic acetylcholine receptor; SCAM, substituted cysteine accessibility method.

Molecular Pharmacology Fast Forward. Published on September 27, 2005 as DOI: 10.1124/mol.105.015164
This article has not been copyedited and formatted. The final version may differ from this version.

Abstract

We have previously shown that the function of neuronal nicotinic acetylcholine receptors can be modulated by zinc. This modulation varies from potentiation to inhibition, depending on receptor subunit composition and zinc concentration, with the α4β2 and α4β4 receptors displaying the most dramatic potentiation. Here we use site directed mutagenesis to identify glutamate 59 and histidine 162 on the rat α4 subunit as potential mediators of zinc potentiation. By modeling the extracellular domain of the receptor pentamer, we locate these residues to two subunit-subunit interfaces that alternate with the two acetylcholine-binding interfaces. Substitution of a cysteine at either position allows additional reduction of zinc potentiation upon treatment with the methanethiosulfonate reagents MTSEA-biotin and MTSET. Mutagenesis and methanethiosulfonate treatment are most effective at position 162 and the presence of zinc hinders the reaction of MTSEA-biotin with the substituted cysteine at this position, suggesting that α4H162 participates in forming a coordination site for zinc. Mutagenesis and methanethiosulfonate treatment are less effective at position 59, suggesting that while α4E59 may be near the zinc coordination site, it may not be participating in coordination of the zinc ion. Interestingly, the position of α4E59 within the neuronal nAChR is identical to that of a residue that lines the benzodiazepine-binding site on $GABA_A$ receptors. We suggest that the zinc potentiation sites on neuronal nAChRs are structurally and functionally similar to the benzodiazepine-binding sites on $GABA_A$ receptors.

Molecular Pharmacology Fast Forward. Published on September 27, 2005 as DOI: 10.1124/mol.105.015164
This article has not been copyedited and formatted. The final version may differ from this version.

Nicotinic acetylcholine receptors (nAChRs) belong to a family of neurotransmitter receptors that includes GABA, glycine and serotonin gated ion channels. Affinity labeling and mutagenesis studies suggest that agonist-binding sites on these pentameric receptors are located at interfaces between subunits (Corringer et al., 2000). On muscle nAChRs, agonist binding sites are located at the interfaces between the αγ and αδ subunit pairs, with the α subunits contributing a "principal component" of several amino acid sequence segments (A, B, C) and the γ/δ subunits contributing a "complementary component" of several segments (D, E, F) (Corringer et al., 2000). The structure of the acetycholine binding protein (AChBP) confirms this model (Brejc et al., 2001; Smit et al., 2001; Celie et al., 2004). The AChBP homopentamer binds agonist at all five interfaces, with each AChBP monomer supplying the "principal" contribution to one binding site and the "complementary" contribution to another binding site. Some neuronal nAChRs are also homopentamers (α7) and form agonist-binding sites in a similar manner (Corringer et al., 1995). However, many neuronal nAChRs are heteromeric with some subunits making the "principal" contribution (α2-α4, α6) and others making the "complementary" contribution (β2, β4) (Corringer et al., 2000). For these receptors, the formation of an agonist-binding site at the interface between two dissimilar subunits, and the rotational symmetry revealed by the AChBP structure, limits the number of agonist binding sites to two. This raises an interesting question. If only two interfaces are involved in binding agonist, what is the function of the other interfaces?

Ionic zinc is found in neurons throughout the brain, with highest concentrations in the cerebral cortex and limbic areas (Frederickson et al., 2000). Zn^{2+} is packaged in synaptic vesicles and released upon neuronal stimulation in a calcium dependent manner (Assaf and Chung, 1984; Howell et al., 1984). Estimates of extracellular [Zn^{2+}] during neuronal activity vary from 10-40 μM (Li et al., 2001) to 100-300 μM (Assaf and Chung, 1984; Vogt et al., 2000). Zn^{2+} modulates the function of neuronal nAChRs

Molecular Pharmacology Fast Forward. Published on September 27, 2005 as DOI: 10.1124/mol.105.015164
This article has not been copyedited and formatted. The final version may differ from this version.

(Palma et al., 1998; Garcia-Colunga et al., 2001; Hsiao et al., 2001) and other ligand gated ion channels (Huang, 1997), suggesting that Zn^{2+} is a modulator of synaptic activity. Indeed, synaptically released Zn^{2+} modulates synaptic activity in the hippocampus (Vogt et al., 2000; Ueno et al., 2002).

Some neuronal nAChRs, such as $\alpha4\beta2$ and $\alpha4\beta4$, are potentiated by micromolar Zn^{2+} and inhibited by millimolar Zn^{2+} (Hsiao et al., 2001). Others, such as $\alpha3\beta2$ (Hsiao et al., 2001) and $\alpha7$ (Palma et al., 1998), are only inhibited by Zn^{2+}. Results with chimeric receptor subunits, and the sensitivity of potentiation to diethylpyrocarbonate and changes in pH, indicate that extracellular histidines participate in forming the potentiating Zn^{2+} binding site(s) (Hsiao et al., 2001). Here we combine conventional mutagenesis, the substituted cysteine accessibility method (SCAM) and protein modeling to identify residues that are determinants of Zn^{2+} potentiation. Our results suggest that neuronal nAChRs bind ACh and Zn^{2+} at alternating subunit-subunit interfaces.

Molecular Pharmacology Fast Forward. Published on September 27, 2005 as DOI: 10.1124/mol.105.015164
This article has not been copyedited and formatted. The final version may differ from this version.

Materials and Methods

Molecular biology. Mutations were introduced into rat neuronal nAChR subunits using the GeneEditor *in vitro* Site-Directed Mutagenesis System (Promega, Madison, WI). All mutations were confirmed by sequencing. Capped cRNA encoding wild-type and mutant subunits was generated using mMessage mMachine kits (Ambion, The Woodlands, TX).

Preparation of oocytes and cRNA injection. Oocytes were surgically removed from mature *Xenopus laevis* frogs (Nasco, Fort Atkinson, WI). The care and use of *X. laevis* frogs in this study were approved by the University of Miami Animal Research Committee and meet the guidelines of the National Institutes of Health. Follicle cells were removed by treatment with Collagenase B (Boehringer Mannhem, Indianapolis, IN) for 2 hours at room temperature. Stage V oocytes were injected with 0.5 - 10 ng of each cRNA (at a molar ratio of 1:1) in 15 – 50 nl of water and incubated at 18°C in Barth's saline (in mM: 88 NaCl, 1 KCl, 2.4 $NaHCO_3$, 0.3 $CaNO_3$, 0.41 $CaCl_2$, 0.82 $MgSO_4$, 15 HEPES, pH 7.6 and 100μg/ml gentamicin) for 2-7 days.

Electrophysiology and data analysis. Current responses were measured under two-electrode voltage clamp, at a holding potential of –70mV, using TEV-200 voltage clamp units (Dagan, Minneapolis, MN). Micropipettes were filled with 3M KCl and had resistances of 0.3-2.0 MΩ. Current responses, filtered (8-pole, Bessel low pass) at 20 Hz (-3db) and sampled at 100 Hz, were captured, stored and analyzed using a Digidata 1322A (Molecular Devices, Union City, CA) in conjunction with either a Macintosh G3 computer running *AXOGRAPH 4.6* software (Molecular Devices) or a Pentium III PC running *PCLAMP 8* (Molecular Devices). Oocytes were perfused at room temperature (20°-25°C), in chamber constructed from 1/8" inner diameter Tygon tubing, with perfusion solution (in mM: 115 NaCl, 1.8

Molecular Pharmacology Fast Forward. Published on September 27, 2005 as DOI: 10.1124/mol.105.015164
This article has not been copyedited and formatted. The final version may differ from this version.

$CaCl_2$, 2.5 KCl, 0.0001 atropine, 10 HEPES, pH7.2). Perfusion was continuous (except during MTSEA-biotin applications) at a rate of ~4 ml/min. ACh alone and in combination with Zn^{2+} was applied diluted in perfusion solution. Some experiments were conducted using an OpusXpress 6000A Parallel Oocyte Voltage Clamp system running *OPUSXPRESS 1.1* and *CLAMPFIT 9.1* software (Molecular Devices). In these experiments, all perfusion and application of ACh and Zn^{2+} was handled by the OpusXpress system. All Zn^{2+} containing solutions were freshly prepared from a 1 M stock of $Zn(CH_3COO)_2$. In previous work, no difference was seen between the effects of $Zn(CH_3COO)_2$ and $ZnCl_2$ containing solutions (Hsiao et al., 2001). Xenopus oocytes express a Ca^{++}-activated Cl^- channel that can contribute to the whole cell current responses when Ca^{++} permeable channels, such as neuronal nAChRs, are activated. In previous work (Hsiao et al., 2001), we found that the extent of zinc potentiation did not vary across a range of holding potentials (–90 mV to –40 mV). Because the Cl^- channel current amplitude varies dramatically over this voltage range, our results led us to conclude that the Ca^{++}-activated Cl^- channel does not underlie or affect measurement of zinc potentiation of neuronal nAChRs expressed in *Xenopus* oocytes. For this reason we have chosen not to attempt to inhibit the Ca^{++}-activated Cl^- channel.

Wild-type and mutant α4β4 receptors displayed little or no desensitization in response to the low ACh concentrations used here, allowing measurement of Zn^{2+} potentiation as follows. Control current in response to ACh was determined from a 1 sec average beginning 29 sec after initiation of agonist application and compared to a 1 sec average of baseline current immediately prior to ACh application. Current levels during Zn^{2+} co-application were determined from a 1 sec average beginning 29 sec after initiation of Zn^{2+} application and compared to the control current. Potentiation of wild-type α4β4 and all mutants (with one exception, see below) was determined with 1 μM ACh, which lies between the EC_1 and EC_6 for each receptor. We have previously found that the extent of zinc potentiation of wild-

Molecular Pharmacology Fast Forward. Published on September 27, 2005 as DOI: 10.1124/mol.105.015164
This article has not been copyedited and formatted. The final version may differ from this version.

type α4β4 does not vary across this portion of the ACh dose-response curve (Hsiao et al., 2001). For one mutant (α4-2E59C β4C75S), 1 μM ACh was the $EC_{0.2}$. For this receptor, we used 5 μM ACh (the EC_2) to test potentiation.

Wild-type and mutant α4β2 receptors displayed substantial desensitization upon exposure to ACh, requiring measurement of potentiation or inhibition as previously described (Hsiao et al., 2001). Briefly, the initial 30 sec ACh response in the absence of Zn^{2+} was fit to a single exponential decay function. This fit was projected over the next 30 sec during which both ACh and Zn^{2+} were co-applied. The degree of modulation was measured by taking a 1 sec average 29 sec after initiation of Zn^{2+} application and comparing it to a 1 sec average of the projected response to ACh alone during the same time period. Thus, both Zn^{2+} and control values were taken 59 sec after the initiation of the experiment. Potentiation of wild-type α4β2 and all mutants was determined with 10 μM ACh, which lies between the EC_{14} and EC_{24} for each receptor. We have previously found that the extent of zinc potentiation of wild-type α4β2 does not vary across this portion of the ACh dose-response curve (Hsiao et al., 2001). A similar extent of potentiation was also seen at the lower ACh concentration of 3 μM (the EC_3) (Hsiao et al., 2001).

In the SCAM experiments in Figure 4A-C, Zn^{2+} potentiation was measured before and after a 2-minute incubation with 2mM MTSEA-biotin (Toronto Research Chemicals, Inc., North York, Ontario, Canada). MTSEA-biotin was diluted from a DMSO stock solution into perfusion solution immediately prior to application. The final DMSO concentration of 0.5% had no effect on ACh responses or zinc potentiation (data not shown). Following the incubation, oocytes were rinsed for 5 minutes with perfusion solution prior to measuring Zn^{2+} potentiation. The high concentration of MTSEA-biotin and relatively long duration of the incubation were chosen to ensure saturation. Indeed, application of fresh

Molecular Pharmacology Fast Forward. Published on September 27, 2005 as DOI: 10.1124/mol.105.015164
This article has not been copyedited and formatted. The final version may differ from this version.

reagent for a further 5 min incubation failed to cause any further loss of potentiation (data not shown). In some experiments, 1 mM MTSET was used.

In the SCAM reaction rate experiments in Figure 4D, potentiation of the response of α4-2H162C β4C75S to 1 μM ACh by 100 μM Zn^{2+} was measured using our standard protocol. 1 μM MTSEA-biotin was then applied for 5 seconds. The oocytes were then rinsed for 5 minutes and potentiation was measured again. This process was repeated and the cumulative exposure times used to determine the reaction rates in the presence and absence of 100 μM Zn^{2+}. The concentration of MTSEA-biotin (1 μM) that would yield a measurable reaction rate was determined empirically. Reaction rates were determined by fitting to the single exponential decay equation: $Y = Y_{max}e^{-kt}$, where Y is the potentiation at time t (in seconds), Y_{max} is the initial potentiation and k is the pseudo-first-order rate constant. The second-order rate constant was obtained by dividing k by the concentration of MTSEA-biotin (Pascual and Karlin, 1998).

Both ACh and Zn^{2+} dose-response curves were fit according to the equation: $I = I_{max}/(1+(EC_{50}/X)^n)$ where I represents the current response at a given concentration of ACh or Zn^{2+}, X; I_{max} is the maximal response; EC_{50} is the concentration of ACh or Zn^{2+} yielding a half maximal response; n is the Hill coefficient. Zinc inhibition data (see Results) was fit according to the equation: $I = I_{max}/(1+(X/IC_{50})^n)$ where *I* represents the current response at a given metal concentration, *X*; I_{max} is the maximal current; IC_{50} is the concentrations of metal yielding half-maximal inhibition; *n* is the Hill coefficient. Data presented in Figure 3B was fit to a more complex equation that included both a potentiating and an inhibitory site: $I = I_{min}+(I_{max}-I_{min})\{[1/(1+(EC_{50}/X)^n)]-[1/(1+(IC_{50}/X)^m)]\}$ where *I* represents the current response at a given metal concentration, *X*; I_{min} is the minimal current; I_{max} is the maximal current; EC_{50} and IC_{50} are the concentration of metal yielding half-maximal potentiation and inhibition, respectively; *n* and *m* are the Hill coefficients for potentiation and inhibition, respectively.

Molecular Pharmacology Fast Forward. Published on September 27, 2005 as DOI: 10.1124/mol.105.015164
This article has not been copyedited and formatted. The final version may differ from this version.

Data analysis was performed using *PRISM 3* software (GraphPad, San Diego, CA). Statistical significance was assessed using a two-tailed unpaired t-test, or a one-way ANOVA followed by the Dunnett's post-test, as appropriate.

Molecular modeling. Sequence alignment of the amino-terminal extracellular region of the rat α4 and β4 neuronal nAChR subunits with the AChBP was performed using the *ALIGNX* module of *VECTOR NTI 5* (InforMax, Inc., No. Bethesda, Maryland). The alignments between the AChBP and α4 and β4 had identity values of 20.4 and 19.4%, respectively. While the sequence identity between the AChBP monomer and amino-terminal extracellular domains of various nAChR subunits is relatively low, the presence of highly conserved ACh binding residues in the AChBP (Brejc et al., 2001) and the nicotinic pharmacology of the AChBP (Smit et al., 2001) suggests that homology modeling of neuronal nAChR extracellular domains using the AChBP structure is appropriate (Le Novere et al., 2002).

Three-dimensional models were constructed using the program *MODELLER 6* (Sali and Blundell, 1993) on a Silicon Graphics Indigo2 Extreme workstation. The script "model" was used with neuronal nAChR subunit / AChBP alignments. Disulfide bonds in the AChBP template structure were explicitly included during homology model refinement. The amino-terminal extracellular domain sequences of the α4 and β4 subunits were modeled using the AChBP pentamer structure (Brejc et al., 2001) (PDB ID: 1I9B) to get initial coordinates for an α4β4 pentamer (subunit ordering of αβαββ). Ten models were produced with energy refinement handled within the program. Conditions were optimized such that resulting structures exhibited energies in line with current published nicotinic receptor homology models (Le Novere et al., 2002; Everhart et al., 2003). The lowest energy structure was then inspected visually and with *PROCHECK* (Laskowski et al., 1993) for inappropriate stereochemistry (clashing side chains, disallowed torsion angles, etc.). In only one case, did a residue

Molecular Pharmacology Fast Forward. Published on September 27, 2005 as DOI: 10.1124/mol.105.015164
This article has not been copyedited and formatted. The final version may differ from this version.

require manual adjustment using the *O* software package (Jones et al., 1991). Further minimization was then carried out using the *CNS* software package (Brünger, 1998), with twenty cycles of conjugate gradient. The *CNS* minimized structure was then reanalyzed with *PROCHECK* to ensure stereochemical soundness. The images in Figures 1B and 6 were produced using *RIBBONS* (Carson, 1997). Coordinates for the final α4β4 model may be obtained at http://chroma.med.miami.edu/pharm/faculty_Luetje.html.

Molecular Pharmacology Fast Forward. Published on September 27, 2005 as DOI: 10.1124/mol.105.015164
This article has not been copyedited and formatted. The final version may differ from this version.

Results

The effect of 100 μM Zn^{2+} on current responses induced by low concentrations of ACh varies from inhibition of α3β2 receptors to greater than 5-fold potentiation of α4β4 receptors, with the α3β4 and α4β2 receptors displaying intermediate levels of potentiation (Figure 1A). The large difference in the effect of Zn^{2+} on α4β4 and α3β2 receptors suggested a strategy for identifying the site at which Zn^{2+} binds and potentiates neuronal nAChRs; mutagenesis of residues present in α4 and β4, but not in α3 and β2.

Amino acid residues that most commonly form Zn^{2+}-binding sites include histidines, free cysteines, aspartates and glutamates (Glusker, 1991). Our previous work indicated the involvement of extracellular histidine residues (Hsiao et al., 2001) and so we used site-directed mutagenesis to test the role of the seven histidine residues unique to the extracellular portions of α4 and β4. We also examined the two unique extracellular free cysteine residues. Our screen included five residues within the amino-terminal extracellular domain of α4 (H2, H61, H104, H109, H162), two residues within this region of β4 (C75, H157), one residue within the carboxy-terminal extracellular portion of α4 (C594) and one residue within the carboxy-terminal extracellular portion of β4 (H469). At some positions, the residue was changed to the residue present at that position in α3 or β2, as appropriate. For α4H2, α4H104 and β4C75 the residues present in α3 and β2 might also be Zn^{2+}-coordinating (glutamate, aspartate and aspartate, respectively). Thus, in addition to testing α4H2E and α4H104D mutants, we also tested the alanine mutants, α4H2A and α4H104A. For β4C75, we tested a serine mutant. To test the role of α4C594, we used a naturally occurring splice variant (α4-2), which lacks this C-terminal cysteine (Goldman et al., 1987). The positions of these residues within an alignment of α3, α4, β2 and β4 are shown in Figure 1C. To visualize the positions of these residues within the receptor structure we

Molecular Pharmacology Fast Forward. Published on September 27, 2005 as DOI: 10.1124/mol.105.015164
This article has not been copyedited and formatted. The final version may differ from this version.

generated a homology model of the extracellular domain of the $(\alpha4)_2(\beta4)_3$ pentamer, using the AChBP (Brejc et al., 2001) as a template structure (see Materials and Methods). Many of these residues are located at the non-ACh-binding subunit-subunit interfaces within the pentamer (Figure 1B).

We used the α4β4 receptor as our primary target to allow analysis of α4 and β4 residues in the same receptor. The α4β4 receptor is also convenient because it displays the greatest degree of zinc potentiation, expresses well in oocytes and shows little or no desensitization in response to low ACh concentrations. The role of critical residues in α4 was also confirmed with α4β2 (see below), a major nAChR subtype in the mammalian CNS (Corringer et al., 2000). Mutant α4 and β4 subunits were coexpressed in *Xenopus* oocytes with wild-type β4 or α4 subunits, respectively. ACh dose-response curves, constructed for each mutant receptor, showed that the mutations had little or no effect on ACh sensitivity (Table 1). We used 100 μM Zn^{2+} to test the effect of each mutation because 100 μM Zn^{2+} lies at the peak of the biphasic potentiation-inhibition curve for α4β4 (Hsiao et al., 2001). Thus, reductions in maximal potentiation, or shifts in the curve would be detected. When compared to wild-type α4β4 receptors, some mutant receptors (such as α4H162Gβ4) displayed reduced potentiation by 100 μM Zn^{2+} (45±4% of wild-type), while others (such as α4β4C75S) displayed potentiation similar to that of wild-type α4β4 (Figure 2A). In addition to α4H162G, the α4H61N and β4H469Y mutations also caused significant decreases in potentiation by 100 μM Zn^{2+} (Figure 2B, Table 2). The α4-2β4 receptor (which lacks the C-terminal cysteine) displayed an increase in potentiation, suggesting potential involvement in the allosteric pathway. However, because we are focused on identifying the zinc potentiation site, we chose not to pursue this possibility. In our model of the α4β4 extracellular domain, the side chains of β4D195 and α4E59 are near the side chain of α4H162 (Figure 1B). Because D195 is conserved in both the β2 and β4 subunits, we substituted an alanine at this position. We also prepared a α4E59A mutant. The α4E59Aβ4 receptor displayed significantly reduced potentiation by 100 μM Zn^{2+},

Molecular Pharmacology Fast Forward. Published on September 27, 2005 as DOI: 10.1124/mol.105.015164
This article has not been copyedited and formatted. The final version may differ from this version.

while the α4β4D195A receptor did not differ from wild type α4β4 (Figure 2B). The results of this mutagenesis screen identifies α4E59, α4H61, α4H162 and β4H469 as candidates for involvement in forming the zinc potentiation site.

In Figure 3A, we examined the effects of a range of zinc concentrations on wild type and mutant α4β4 receptors. The α4E59A, α4H61N, α4H162G and β4H469Y mutations each reduced maximal potentiation by Zn^{2+}, but none of the mutations increased the EC_{50} for zinc potentiation, as might be expected if the mutations were damaging a zinc-binding site (Table 2). However, a simple rightward shift in the zinc dose-response curve could be expected only if zinc potentiation were occurring in isolation. We have previously shown that zinc both potentiates and inhibits these receptors at separate sites. At and above 300 μM Zn^{2+}, receptor inhibition of the α4β4 receptor becomes apparent, leading to a distinctly biphasic Zn^{2+} dose-response curve (Hsiao et al., 2001). If the mutations were causing damage to the potentiation site, while leaving the inhibition site intact, a rightward shift in the potentiation curve could be obscured.

To investigate this issue in more detail, we examined the effects of a wider range of Zn^{2+} concentrations on the α4H162Gβ4 mutant (Figure 3B). Obtaining accurate values from fitting biphasic zinc dose-response data to a two-site equation is difficult due to the close proximity of potentiating and inhibiting phases (Hsiao et al., 2001). However, in this earlier study we found that diethylpyrocarbonate (DEPC) treatment eliminates potentiation, without affecting inhibition, of the α4β4 receptor. We fit this data to a single site inhibition equation to obtain an IC_{50} for Zn^{2+} inhibition of 362 ± 70 μM (see Materials and Methods). We then fit the biphasic zinc dose-response data for wild-type α4β4 in our earlier study to a two-site equation (see Materials and Methods) using this IC_{50} value as a constant. This allowed us to estimate parameters for zinc potentiation of the wild type α4β4 receptor (EC_{50} = 110 ± 33 μM, n_H = 0.96 ± 0.04, Maximal Potentiation = 1400 ± 250%). The EC_{50} value is 4-fold greater and the

Molecular Pharmacology Fast Forward. Published on September 27, 2005 as DOI: 10.1124/mol.105.015164
This article has not been copyedited and formatted. The final version may differ from this version.

maximal potentiation value 2-fold greater than what we obtain when we fit the potentiating phase of the data to a single site equation. This suggests that the inhibiting phase does indeed partially obscure the potentiation phase. Because zinc inhibition occurs at a separate class of site (Hsiao et al., 2001), it is unlikely to be affected by mutations at the zinc potentiation site. This allows us to use the inhibition parameters obtained from fitting the post-DEPC treatment wild-type α4β4 receptor when fitting the data obtained for the α4H162Gβ4 mutant. If we also assume that maximal potentiation is not changing, we find that upon fitting to a two site equation, the EC_{50} for zinc potentiation of the α4H162Gβ4 mutant is greater (267 ± 7 μM) than the value for wild type α4β4. This analysis suggests, but does not prove, that the α4H162Gβ4 receptor is indeed less sensitive to zinc potentiation than wild type α4β4. In order to prove this conclusively using dose-response analysis, we would need to be able to examine potentiation in the absence of inhibition. However, we have been unable to eliminate, or even damage, the inhibition of nAChRs by zinc (Hsiao et al., 2001). None of the mutations we have examined reduce inhibition by high concentrations of zinc (data not shown). Thus, we turned to other approaches to provide additional information about the role of candidate residues in forming the zinc potentiation site.

First, we examined the effect of double mutant combinations, reasoning that simultaneous mutation of two residues involved in mediating zinc potentiation should yield an effect greater than with either single mutation. Because the α4H162G mutant displayed the greatest loss of Zn^{2+} potentiation, we used this receptor as a point of reference. Each of the other 3 mutations was examined as a double mutant with α4H162G. The α4H61N and β4H469Y mutations failed to alter potentiation of the α4H162G β4 receptor. Potentiation of these double mutants by 100μM Zn^{2+} was 107±7% and 99±7% of the potentiation of the α4H162G single mutant, respectively. This result suggests that these residues might not play important roles in mediating Zn^{2+} potentiation. In contrast, receptors formed by the double mutant α4E59A, H162G displayed significantly decreased potentiation when compared to the

Molecular Pharmacology Fast Forward. Published on September 27, 2005 as DOI: 10.1124/mol.105.015164
This article has not been copyedited and formatted. The final version may differ from this version.

potentiation of α4H162G (81±5% of the single mutant potentiation, $p<0.05$, n=13). Interestingly, potentiation was not completely eliminated. Receptors formed by the α4E59A, H162G double mutant retained a modest ability to be potentiated by Zn^{2+} (36% of wild-type, see discussion).

As an alternative approach to testing the role of candidate residues in forming a zinc potentiation site, we turned to the substituted cysteine accessibility method (SCAM) (Karlin and Akabas, 1998). In SCAM analysis, a cysteine is placed at the position of interest and function is then measured before and after reaction with a methanethiosulfonate (MTS) reagent. While free cysteines can participate in coordination of Zn^{2+}, they often do not substitute effectively for other coordinating residues (Paoletti et al., 2000). This is most likely due to stringent spatial requirements for the relevant atoms (S, N and O) to be able to coordinate the zinc ion. The result of our double mutant experiments (see above) suggest that even if a substituted cysteine failed to directly participate in Zn^{2+} coordination (thus constituting a single mutant), the functional damage to the site would be partial. A further reduction of Zn^{2+} potentiation after reaction with an MTS reagent would then suggest a physical proximity to the zinc ion and would strengthen the case for direct coordination. As the MTS reagent for most of our experiments, we used MTSEA-biotin, a large, relatively membrane impermeant MTS reagent that has been used to characterize various sites on $GABA_A$ receptors (Teissere and Czajkowski, 2001; Wagner and Czajkowski, 2001). To avoid the potential for confounding effects of the MTS reagent acting at other free cysteines, the α4-2 β4C75S mutant receptor, which lacks extracellular free cysteine residues, was used as a "pseudo-wild-type" background (Karlin and Akabas, 1998) in which to test each cysteine mutant. This pseudo-wild-type receptor displayed ACh sensitivity and Zn^{2+} potentiation similar to that of true wild-type α4β4 and was unaffected by MTSEA-biotin treatment (Tables 1 and 2, Figure 4A and C).

Molecular Pharmacology Fast Forward. Published on September 27, 2005 as DOI: 10.1124/mol.105.015164
This article has not been copyedited and formatted. The final version may differ from this version.

We prepared E59C, H61C and H162C mutants, each within the context of the pseudo-wild-type receptor. Each mutation resulted in significantly reduced Zn^{2+} potentiation (61±5%, 63±9% and 77±2% of pseudo-wild-type potentiation, respectively), similar to what was seen with the E59A, H61N and H162G mutations. MTSEA-biotin treatment (2 mM, 2 min) had no significant effect on the ACh responses of any of the mutant receptors (data not shown). MTSEA-biotin also had no effect on Zn^{2+} potentiation of the α4H61C receptor (Figure 4C), again suggesting that α4H61 may not play an important role in mediating Zn^{2+} potentiation. In contrast, MTSEA-biotin treatment significantly reduced potentiation of the α4E59C and α4H162C receptors, suggesting that α4E59 and α4H162 are located at or near the Zn^{2+}-binding site (Figure 4B and C). However, as was the case for the double mutant, these MTSEA-biotin treated mutant receptors retained some ability to be potentiated by Zn^{2+}. In Figure 4, we used 1 μM ACh to test potentiation of the pseudo-wild-type receptor, as well as the α4H61C and α4H162C receptors. However, we used the equipotent concentration of 5 μM ACh to test potentiation of the α4E59C (see Materials and Methods). We also tested the ability of MTSEA-biotin to reduce zinc potentiation of the α4E59C using 1μM ACh, finding post-treatment potentiation to be 76 ± 4% of pre-treatment potentiation ($p<0.05$, $n=6$). Zinc potentiation could also be reduced by MTSET application (1 mM, 2 min). While the trimethylammonium ethyl group deposited by MTSET is substantially smaller than the biotinylaminoethyl group deposited by MTSEA-biotin, it does have a positive charge that would be likely to interfere with Zn^{2+} binding. Post-treatment potentiation of α4-2H162C β4C75S by 100 μM Zn^{2+} was 71 ± 3% of pretreatment potentiation ($n = 6$, $p < 0.001$) and for α4-2E59C β4C75S the value was 83 ± 3% of pretreatment potentiation ($n = 3$, $p < 0.05$). The effects of MTSEA-biotin and MTSET on zinc potentiation of the α4E59C mutant were substantially less than the effects on the α4H162C mutant. This may be due, in part, to fact that substituting a cysteine for α4E59 had a greater effect on zinc potentiation than did substitution of α4H162 (61±5% and 77±2% remaining

Molecular Pharmacology Fast Forward. Published on September 27, 2005 as DOI: 10.1124/mol.105.015164
This article has not been copyedited and formatted. The final version may differ from this version.

potentiation, respectively). Thus, there is less remaining potentiation to be affected by the MTS reagent. However, it is also possible that while α4E59 may be near the site of zinc binding, it might not be directly participating in coordination of the zinc ion.

SCAM can also be used to obtain information about the relative accessibility of a site under different conditions (Karlin and Akabas, 1998). By alternating short exposures to low concentrations of MTS reagent with functional measurements, a reaction rate (and thus a relative measure of accessibility) can be determined (Pascual and Karlin, 1998). In Figure 4D, we use this methodology to examine the relative accessibility for MTSEA-biotin at position 162 of α4 in the presence and absence of Zn^{2+}. Oocytes expressing α4-2H162C β4C75S were exposed to 1 μM MTSEA-biotin in 5 sec increments. After each application, the oocytes were rinsed and the extent of potentiation by 100 μM Zn^{2+} was determined. The decline in Zn^{2+} potentiation upon repeated exposure to MTSEA-biotin was then fit to an exponential decay function. In the absence of Zn^{2+}, the halftime of the reaction was 8.7 sec, yielding a rate of 79,000 ± 14,000 $M^{-1}s^{-1}$. In the presence of 100 μM Zn^{2+}, the halftime of the reaction was 21.3 sec, yielding a rate of 32,000 ± 10,000 $M^{-1}s^{-1}$. Despite the change in reaction rate, the extent of the effect was the same in the presence and absence of Zn^{2+} (the fit plateau was 0.69±0.05 and 0.65±0.02, respectively). The significant decrease in reaction rate ($p<0.01$) indicates that the site is less accessible to MTSEA-biotin when Zn^{2+} is present and suggests that Zn^{2+} is competing with MTSEA-biotin for occupation of the site.

In addition to potentiation of the ACh response, zinc potentiates the response of neuronal nAChRs to nicotine. Potentiation of α4β4 by coapplication of 100 μM Zn^{2+} with 1μM nicotine was 444 ± 43% of the response to nicotine alone. The α4H162G and α4E59A mutant receptors each displayed significantly reduced potentiation by 100 μM Zn^{2+} (50±5% of wild-type α4β4, $p<0.05$ and 88±4% of wild-type α4β4, $p<0.01$, respectively).

Molecular Pharmacology Fast Forward. Published on September 27, 2005 as DOI: 10.1124/mol.105.015164
This article has not been copyedited and formatted. The final version may differ from this version.

We also examined the effect of mutating α4H162 and α4E59 in a different receptor subunit context: α4β2 (Figure 5). The α4β2 is a major nAChR subtype in the CNS (Corringer et al., 2000). The effect of zinc on α4β2 receptors was substantial, with a maximum potentiation of approximately 2.5-fold achieved at 50 μM Zn^{2+} (Figures 1A and 5A, and see Hsiao et al., 2001). The α4E59A and α4H162G mutations were each able to significantly reduce the extent of potentiation by 50 μM Zn^{2+} (Figure 5B).

Molecular Pharmacology Fast Forward. Published on September 27, 2005 as DOI: 10.1124/mol.105.015164
This article has not been copyedited and formatted. The final version may differ from this version.

Discussion

We have identified α4E59 and α4H162 as determinants of Zn^{2+} potentiation on rat neuronal nAChRs. The positions of these residues within our receptor model are shown in Figure 6. A strong case can be made for direct coordination of the zinc ion by α4H162. Mutation of this residue results in a large loss of zinc potentiation, MTSEA-biotin has a substantial effect when a cysteine is at this position and zinc can slow the reaction of MTSEA-biotin with a cysteine at this position. While the side chain on α4E59 is close enough to the side chain of α4H162 (in Figure 1B, the εN of H162 is 5.6 Å from the nearest carboxyl oxygen in E59) for a role in coordination to be plausible (Harding, 2001), the effects of mutation and MTSEA-biotin treatment are substantially less than what is seen at position 162. Thus, while α4H162 is likely to be participating in direct coordination of the zinc ion, α4E59 may only be near the zinc potentiation site without actually participating in zinc coordination.

The location of zinc potentiation sites on neuronal nAChRs

The positions of α4H162 and α4E59 within the receptor and the involvement of both α and β subunits in mediating Zn^{2+} potentiation (Hsiao et al., 2001) suggest that neuronal nAChRs bind Zn^{2+} at subunit-subunit interfaces that alternate with ACh binding interfaces. This depends on our decision to model the receptor with a subunit arrangement of αβαββ. Whether the fifth subunit is β or α is irrelevant. In either case the receptor would have 2 ACh-binding and 2 zinc-binding interfaces. More important is the arrangement of the first 4 subunits in an alternating αβαβ pattern. This arrangement appears to be required. The subunits of the AChBP are arranged in a rotationally symmetric manner, with each subunit supplying a "principal" face to one ACh binding site and a "complementary" face to another ACh binding site (Brejc et al., 2001; Celie et al., 2004). In heteromeric neuronal nAChRs, the "principal" residues are only present on the α subunit, while the "complementary" residues are only

Molecular Pharmacology Fast Forward. Published on September 27, 2005 as DOI: 10.1124/mol.105.015164
This article has not been copyedited and formatted. The final version may differ from this version.

present on the β subunit (Corringer et al., 2000). Thus, both α and β subunits are required to form an ACh binding site. Regardless of whether the α:β stoichiometry is 2:3 or 3:2, only two non-adjacent interfaces will form ACh binding sites. An additional two non-adjacent interfaces would form Zn^{2+}-binding sites.

Neuronal nAChRs also form as homopentamers of the α7 subunit (Corringer et al., 2000). The α7 subunit lacks both H162 and E59 (Le Novere and Changeux, 2001), and α7 homopentamers are thought to bind ACh at all five interfaces (Corringer et al., 2000). As would be expected, α7 homomers are not potentiated by Zn^{2+} (Palma et al., 1998). A novel Zn^{2+}-activated channel (ZAC) has been reported (Davies et al., 2003). This homomeric receptor is structurally homologous to nAChRs. While ZAC subunits have a histidine in a similar position as α4H162, no aspartates or glutamates are located near the position analogous to α4E59. It is unclear if the ZAC binds Zn^{2+} at a site similar to the potentiation site we have identified on neuronal nAChRs.

We have identified at least one residue (α4H162) as part of a pair of identical Zn^{2+} potentiation sites on neuronal nAChRs. Because Zn^{2+}-binding sites can have 4, 5 or 6 coordination points (Glusker, 1991), additional residues remain to be identified. These receptors may also possess a second class of Zn^{2+} potentiation site. In our single mutation experiments, only partial losses of potentiation were observed. This was not unexpected. However, even the double mutant α4E59A, H162G retained a modest ability to be potentiated by Zn^{2+} application (approximately one-third of wild-type potentiation). In our SCAM experiments, we also did not completely eliminate potentiation. This contrasts with the complete elimination of potentiation upon diethypyrocarbonate treatment (Hsiao et al., 2001). Thus, neuronal nAChRs might possess at least three distinct classes of Zn^{2+} binding site, a major potentiation site accounting for roughly 2/3 of the potentiation (identified here), a minor potentiation site accounting for roughly 1/3 of the potentiation and an inhibitory site. Glutamate, GABA and glycine receptors also

Molecular Pharmacology Fast Forward. Published on September 27, 2005 as DOI: 10.1124/mol.105.015164
This article has not been copyedited and formatted. The final version may differ from this version.

possess multiple classes of Zn^{2+} modulatory sites (Paoletti et al., 2000; Laube et al., 2002; Hosie et al., 2003).

Zinc potentiation sites have structural similarities to ACh binding sites

We compared the zinc potentiation site with other binding sites on cys-loop receptors. The ACh binding site on nAChRs has been extensively characterized (Corringer et al., 2000). E59 is located within the "D-loop" region of α4. In an ACh-binding interface, the D-loop is supplied by the γ, δ or ε subunits of muscle nAChRs or the β subunits of neuronal nAChRs and contributes a critical tryptophan residue to the binding site, as well as several determinants of pharmacological diversity (Corringer et al., 2000; Celie et al., 2004). H162 is located within the "F loop" region of α4. At ACh binding interfaces, this region is also supplied by the "non-α" subunits of muscle and neuronal nAChRs and contains determinants of pharmacological diversity (Corringer et al., 2000). Thus, the Zn^{2+}-binding site that we have identified has structural similarity to the ACh binding site.

Zinc potentiation sites are not related to calcium potentiation sites on neuronal nAChRs

Neuronal nAChRs are also potentiated by extracellular Ca^{2+} (Mulle et al., 1992; Vernino et al., 1992). Critical glutamate residues mediating Ca^{2+} potentiation have been identified on α7 (Galzi et al., 1996). These residues are highly conserved among neuronal nAChRs and correspond to α4E45/β4E49 (located between β strands 1 and 2) and α4E175/β4E179 (located just before β strand 9). Both putative Ca^{2+} binding sites are located at the bottom (proximal to the membrane) of the receptor structure shown in Figure 1B, away from the Zn^{2+} potentiation site we have identified. Also, Ca^{2+} potentiation of α4β4 is unaffected by the α4H162G and α4E59A mutations (data not shown). Thus, Zn^{2+} and Ca^{2+} act at separate sites on neuronal nAChRs.

Molecular Pharmacology Fast Forward. Published on September 27, 2005 as DOI: 10.1124/mol.105.015164
This article has not been copyedited and formatted. The final version may differ from this version.

Zinc potentiation sites are not related to zinc binding sites of other ligand gated ion channels

Other cys-loop receptors also possess Zn^{2+}-binding sites. On the glycine receptor α1 subunit, D80 participates in a Zn^{2+}-potentiation site at subunit-subunit interfaces near the top (distal from the cell surface) of the receptor extracellular domain, while H107, H109 and T112 participate in an inhibitory site that faces into the vestibule (Laube et al., 2002). The Zn^{2+} site that we have identified on neuronal nAChRs is not structurally comparable to either of these sites. $GABA_A$ receptors also possess multiple Zn^{2+}-binding sites. For clarity, it is important to remember that $GABA_A$ receptor β subunits are equivalent to neuronal nAChR α subunits, while $GABA_A$ receptor α subunits are equivalent to neuronal nAChR β subunits. Thus, while neuronal nAChRs bind ACh at α-β interfaces, GABA receptors bind GABA at β-α interfaces (Smith and Olsen, 1995). In the α1β3 $GABA_A$ receptor, α1E137, α1H141 and β3E182 participate in a Zn^{2+}-binding inhibitory site located at α-β interfaces (non-GABA binding interfaces) near the bottom (proximal to the cell surface) of the receptor extracellular domain (Hosie et al., 2003). A separate class of Zn^{2+}-binding inhibitory site is located within the ion channel. The Zn^{2+}-potentiation site we have identified on neuronal nAChRs is not structurally comparable to either of these Zn^{2+}-binding sites on $GABA_A$ receptors. Glutamate gated ion channels also possess zinc-binding sites, which have been characterized in detail (Paoletti et al., 2000). However, these receptors are structurally unrelated to nAChRs, precluding a comparison with the Zn^{2+}-potentiation site on neuronal nAChRs.

Zinc potentiation sites are analogous to the benzodiazepine-binding site on $GABA_A$ receptors

The most interesting comparison is with the binding site for benzodiazepines on $GABA_A$ receptors. While GABA binds at β-α interfaces, incorporation of a γ subunit allows benzodiazepines to

Molecular Pharmacology Fast Forward. Published on September 27, 2005 as DOI: 10.1124/mol.105.015164
This article has not been copyedited and formatted. The final version may differ from this version.

bind at the α-γ interface (Smith and Olsen, 1995). A series of residues on the γ2 subunit (Y58, F77, A79, T81) have been identified as components of the benzodiazepine-binding site (Kucken et al., 2000; Teissere and Czajkowski, 2001; Kucken et al., 2003). Examination of aligned amino acid sequences (Le Novere and Changeux, 2001) and a model of the α1β2γ2 $GABA_A$ receptor extracellular domain (Kucken et al., 2003) reveals that the benzodiazepine-binding site residue γ2T81 (Teissere and Czajkowski, 2001) is in a location identical to that of α4E59. While α4E59 may not directly coordinate zinc, it is close to the zinc potentiation site on neuronal nAChRs. This suggests that the binding of agonists and modulators at alternating subunit-subunit interfaces is a general property of heteromeric cys-loop receptors. The similar location of the zinc potentiation sites on neuronal nAChRs and the benzodiazepine binding site on $GABA_A$ receptors, as well as the similar modulatory function of both sites, leads us to suggest that the Zn^{2+} potentiation sites on neuronal nAChRs are structurally and functionally similar to the benzodiazepine binding site on $GABA_A$ receptors. This identifies the Zn^{2+} potentiation site on neuronal nAChRs as a promising target for future drug development.

Molecular Pharmacology Fast Forward. Published on September 27, 2005 as DOI: 10.1124/mol.105.015164
This article has not been copyedited and formatted. The final version may differ from this version.

References

Assaf SY, Chung S-H (1984) Release of endogenous Zn^{2+} from brain tissue during activity. *Nature* 308:734-736.

Brejc K, van Dijk WJ, Klaassen RV, Schuurmans M, van der Oost J, Smit AB, Sixma TK (2001) Crystal structure of an ACh-binding protein reveals the ligand-binding domain of nicotinic receptors. *Nature* 411:269-276.

Brünger AT (1998) Crystallography & NMR System: A new software suite for macromolecular structure determination. *Acta Cryst* D54:905-921.

Carson M (1997) Ribbons. *Methods in Enzymology* 277:493-505.

Celie PHN, van Rossum-Fikkert SE, van Dijk WJ, Brejc K, Smit AB, Sixma TK (2004) Nicotine and caramylcholine binding to nicotinic acetylcholine receptors as studied in AChBP crystal structures. *Neuron* 41:907-914.

Corringer PJ, Le Novere N, Changeux JP (2000) Nicotinic receptors at the amino acid level. *Annu Rev Pharmacol Toxicol* 40:431-458.

Corringer PJ, Galzi JL, Eisele JL, Bertrand S, Changeux JP, Bertrand D (1995) Identification of a new component of the agonist binding site of the nicotinic alpha 7 homooligomeric receptor. *J Biol Chem* 270:11749-11752.

Davies PA, Wang W, Hales TG, Kirkness EF (2003) A novel class of ligand-gated ion channel is activated by Zn^{2+}. *J Biol Chem* 278:721-717.

Everhart D, Reiller E, Mirzoian A, McIntosh JM, Malhotra A, Luetje CW (2003) Identification of residues that confer α-conotoxin PnIA sensitivity on the α3 subunit of neuronal nicotinic acetylcholine receptors. *J Pharmacol Exp Ther* 306:664-670.

Frederickson CJ, Suh SW, Silva D, Frederickson CJ, Thompson RB (2000) Importance of zinc in the central nervous system: the zinc-containing neuron. *J Nutrition* 130:1471S-1483S.

Galzi JL, Bertrand S, Corringer PJ, Changeux JP, Bertrand D (1996) Identification of calcium binding sites that regulate potentiation of a neuronal nicotinic acetylcholine receptor. The EMBO Journal 15:5824-5832.

Garcia-Colunga J, Gonzalez-Herrera M, Miledi R (2001) Modulation of alpha2beta4 neuronal nicotinic acetylcholine receptors by zinc. *Neuroreport* 12:147-150.

Glusker JP (1991) Structural aspects of metal liganding to functional groups in proteins. *Adv Protein Chem* 42:1-76.

Goldman D, Deneris E, Luyten W, Kochhar A, Patrick J, Heinemann S (1987) Members of a nicotinic acetylcholine receptors gene family are expressed in different regions of the mammalian central nervous system. *Cell* 48:965-973.

Harding MM (2001) Geometry of metal-ligand interactions in proteins. *Acta Cryst* D57:401-411.

Hosie AM, Dunne EL, Harvey RJ, Smart TG (2003) Zinc-mediated inhibition of $GABA_A$ receptors: discrete binding sites underlie subtype specificity. *Nature Neurosci* 6:362-369.

Howell GA, Welch MG, Frederickson CJ (1984) Stimulation-induced uptake and release of zinc in hippocampal slices. *Nature* 308:736-738.

Hsiao B, Dweck D, Luetje CW (2001) Subunit-dependent modulation of neuronal nicotinic receptors by zinc. *J Neurosci* 21:1848-1856.

Huang EP (1997) Metal ions and synaptic transmission: think zinc. *Proc Natl Acad Sci USA* 94:13386-13387.

Jones TA, Zou J-Y, Cowan S, Kjeldgaard M (1991) Improved methods for building protein models in electron density maps and the location of errors in these models. *Acta Cryst* A47:110-119.

Karlin A, Akabas MH (1998) Substituted-cysteine accessibility method. *Methods Enzymol* 293:123-145.

Kucken AM, Teissere JA, Seffinga-Clark J, Wagner DA, Czajkowski C (2003) Structural requirements for imidazobenzodiazepine binding to $GABA_A$ receptors. Molec Pharmacol 63:289-296.

Kucken AM, Wagner DA, Ward PR, Teissere JA, Boileau AJ, Czajkowski C (2000) Identification of benzodiazepine binding residues in the γ2 subunit of the γ-aminobutyric $acid_A$ receptor. *Molec Pharmacol* 57:932-939.

Laskowski RA, MacArthur MW, Moss DS, Thornton JM (1993) PROCHECK: a program to check the stereochemical quality of protein structures. *J Appl Cryst* 26:283-291.

Laube B, Maksay G, Schemm R, Betz H (2002) Modulation of glycine receptor function: a novel approach for therapeutic intervention at inhibitory synapses. *Trends Pharmacol Sci* 23:519-527.

Le Novere N, Changeux J-P (2001) LGICdb: the ligand-gated ion channel database. *Nucleic Acids Res* 29:294-295.

Le Novere N, Grutter T, Changeux J-P (2002) Models of the extracellular domain of the nicotinic receptors and of agonist- and Ca^{2+}-binding sites. *Proc Natl Acad Sci USA* 99:3210-3215.

Li Y, Hough CJ, Suh SW, Sarvey JM, Frederickson CJ (2001) Rapid translocation of Zn^{2+} from presynaptic terminals into postsynaptic hippocampal neurons after physiological stimulation. *J Neurophysiol* 86:2597-2604.

Mulle C, Choquet D, Korn H, Changeux JP (1992) Calcium influx through nicotinic receptors in rat central neurons: its relevance to cellular regulation. Neuron 8:937-945.

Palma E, Maggi L, Miledi R, Eusebi F (1998) Effects of Zn^{2+} on wild and mutant neuronal α7 nicotinic receptors. *Proc Natl Acad Sci USA* 95:10246-10250.

Paoletti P, Perin-Dureau F, Fayyazuddin A, Le Goff A, Callebaut I, Neyton J (2000) Molecular organization of a zinc binding N-terminal modulatory domain in a NMDA receptor subunit. *Neuron* 28:911-925.

Pascual JM, Karlin A (1998) State-dependent accessibility and electrostatic potential in the channel of the acetylcholine receptor. *J Gen Physiol* 111: 717-739.

Sali A, Blundell TL (1993) Comparative protein modeling by satisfaction of spatial restraints. *J Mol Biol* 234:779-815.

Smit AB, Syed NI, Schaap D, van Minnen J, Klumperman J, Kits KS, Lodder H, van der Schors RC, van Elk R, Sorgedrager B, Brejc K, Sixma TK, Geraerts WPM (2001) A glia-derived acetylcholine-binding protein that modulates synaptic transmission. *Nature* 411:261-268.

Smith GB, Olsen RW (1995) Functional domains of $GABA_A$ receptors. *Trends Pharmacol Sci* 16:162-168.

Teissere JA, Czajkowski C (2001) A β-strand in the γ2 subunit lines the benzodiazepine binding site of the $GABA_A$ receptor: Structural rearrangements detected during channel gating. *J Neurosci* 21:4977-4986.

Ueno S, Tsukamoto M, Hirano T, Kikuchi K, Yamada MK, Nishiyama N, Nagano T, Matsuki N, Ikegaya Y (2002) Mossy fiber Zn^{2+} spillover modulates heterosynaptic N-methyl-D-aspartate receptor activity in hippocampal CA3 circuits. *J Cell Biol* 158:215-220.

Vernino S, Amador M, Luetje CW, Patrick J, Dani JA (1992) Calcium modulation and high calcium permeability of neuronal nicotinic acetylcholine receptors. Neuron 8:127-134.

Vogt K, Mellor J, Tong G, Nicoll R (2000) The actions of synaptically released zinc in hippocampal mossy fiber synapses. *Neuron* 26:187-196.

Wagner DA, Czajkowski C (2001) Structure and dynamics of the GABA binding pocket: A narrowing cleft that constricts during activation. *J Neurosci* 21:67-74.

Molecular Pharmacology Fast Forward. Published on September 27, 2005 as DOI: 10.1124/mol.105.015164
This article has not been copyedited and formatted. The final version may differ from this version.

Footnotes

This work was supported by NIH grants MH66038 and DA08102 to C.W.L., and GM069972 to A.M. A.M. was supported in part by awards from the Florida Biomedical Research Foundation (BM030), and the American Heart Association, Florida/Puerto Rico Affiliate (SDG-0130456B). B.H., K.B.M., D.E. and S.E.R. were supported in part by T32 HL07188. B.H. was supported in part by a PhRMA Foundation Medical Student Research Fellowship and is a Lois Pope LIFE Fellow.

Send Reprint Requests to:

Charles W. Luetje, Ph.D.
Molecular and Cellular Pharmacology, R-189
University of Miami
P.O. Box 016189
Miami, FL 33101
cluetje@chroma.med.miami.edu

1) B.H and K.B.M. contributed equally to this work.

Molecular Pharmacology Fast Forward. Published on September 27, 2005 as DOI: 10.1124/mol.105.015164
This article has not been copyedited and formatted. The final version may differ from this version.

Figure Legends

Figure 1. **A**, The effect of Zn^{2+} varies with receptor subunit composition. ACh induced current responses of oocytes expressing the indicated neuronal nAChRs before, during and after coapplication of 100 μM Zn^{2+}. ACh concentrations for each receptor are α3β2 = 4 μM (EC_{10}), α3β4 = 17 μM (EC_2), α4β2 = 10 μM (EC_{14}), α4β4 = 1 μM (EC_2). Scale bars: 250 nA, 10 sec. **B**, Two subunits, β4 (blue) and α4 (green), taken from our homology model of the pentameric α4β4 receptor extracellular domain are shown. Residues tested in this study are indicated in red. α4C594 and β4H469 are not shown because they are not within the homology model. **C**, Alignment of the N-terminal extracellular domains (preceding transmembrane I) of α4, α3, β4 and β2, and the C-terminal extracellular tails (following transmembrane IV) of α4-1, α4-2, α3, β4 and β2. Residues tested in this study are indicated in red.

Figure 2. Mutation analysis to identify candidate Zn^{2+} coordinating residues. **A**, Current responses of oocytes expressing wild-type α4β4 (left), α4β4C75S (center) or α4H162Gβ4 (right) to 1 μM ACh before, during and after coapplication of 100 μM Zn^{2+}. Scale bars are 200 nA and 20 sec for α4β4 and α4H162Gβ4, 100 nA and 20 sec for α4β4C75S. **B**, Potentiation of mutant receptors by 100 μM Zn^{2+}. Results are presented as the ratio of mutant receptor potentiation to the potentiation of wild type receptor in the same batch of oocytes (mean ± SEM, n = 3-14). The ACh concentration for all receptors is 1 μM. Significant differences in Zn^{2+} potentiation as compared to wild-type α4β4 are indicated (***$p<0.001$, **$p<0.01$, *$p<0.05$).

Figure 3. **A**, The effects of a range of zinc concentrations on wild-type α4β4 (open circles), α4E59Aβ4 (filled diamonds), α4H61Nβ4 (filled squares), α4H162Gβ4 (filled circles) and α4β4H469Y (open

Molecular Pharmacology Fast Forward. Published on September 27, 2005 as DOI: 10.1124/mol.105.015164
This article has not been copyedited and formatted. The final version may differ from this version.

diamonds) receptors are plotted as a percentage of the response to 1 μM ACh alone. Values are the mean ± SEM from 3-6 oocytes and are fit to a Hill equation (see Materials and Methods). **B**, The potentiating and inhibiting phases of the action of zinc on α4H162Gβ4 receptors is shown. Values are the mean ± SEM from 3 oocytes and are fit to a dual site Hill equation (see Results for an explanation).

Figure 4. SCAM analysis at the Zn^{2+} potentiation site. **A,** Potentiation of the ACh (1 μM) response of an α4-2β4C75S (pseudo-wild-type) expressing oocyte by 100 μM Zn^{2+} before and after a 2 minute incubation with 2 mM MTSEA-biotin (scale: 100 nA, 10 sec). **B,** Potentiation of the ACh (1 μM) response of an α4-2H162C β4C75S expressing oocyte by 100 μM Zn^{2+} before and after a 2 minute incubation with 2 mM MTSEA-biotin (scale: 100 nA, 10 sec). **C,** Potentiation of the α4E59C, α4H61C, and α4H162C mutants (each expressed within the context of the pseudo-wild-type receptor, α4-2β4C75S) by 100 μM Zn^{2+}, measured after a 2 minute incubation with 2mM MTSEA-biotin, is plotted as a percentage of pre-treatment potentiation (mean ± SEM, n = 3-5). Significant differences from pretreated: *$p< 0.05$, ***$p<0.001$. **D**, Reaction rates for MTSEA-biotin at α4-2H162C β4C75S in the presence and absence of 100 μM Zn^{2+}. Potentiation of the response to 1μM ACh was measured before and after successive 5 sec applications of 1 μM MTSEA-biotin. Results are presented as the ratio of post-treatment potentiation to the initial, pre-treatment potentiation. Values are the mean ± SEM from 3-6 oocytes and are fit to an exponential decay equation (see Materials and Methods).

Figure 5. Mutation of α4E59 or α4H162 decreases zinc potentiation of α4β2 receptors. **A**, Current responses of oocytes expressing wild-type α4β2 (left) or α4H162Gβ2 (right) to 10 μM ACh before, during and after coapplication of 50 μM Zn^{2+}. Scale bars are 2 μA and 10 sec. **B**, Potentiation of mutant receptors by 50 μM Zn^{2+}. Results are presented as the ratio of mutant receptor potentiation to

Molecular Pharmacology Fast Forward. Published on September 27, 2005 as DOI: 10.1124/mol.105.015164
This article has not been copyedited and formatted. The final version may differ from this version.

the potentiation of wild type receptor in the same batch of oocytes (mean ± SEM, n = 13-15). Significant differences in Zn^{2+} potentiation as compared to wild-type α4β2 are indicated ($^{\dagger\dagger\dagger}p<0.001$).

Figure 6. Neuronal nAChRs bind zinc and ACh at alternating subunit-subunit interfaces. **A,** Zinc-binding residues at a β4-α4 interface. Residues α4E59 and α4H162 are shown. **B,** The extracellular domain of the α4β4 pentamer is shown viewed from above. α4 subunits are green, β4 subunits are blue. Side chains of several residues that are conserved features of ACh binding sites (α4- Y93, W149, Y190, Y197; β4- W59) are shown in purple. Side chains of α4E59 and α4H162 are shown in red.

Molecular Pharmacology Fast Forward. Published on September 27, 2005 as DOI: 10.1124/mol.105.015164
This article has not been copyedited and formatted. The final version may differ from this version.

Table 1. ACh sensitivity of wild-type and mutant neuronal nAChRs. EC_{50} and n_H values were determined by fitting to a Hill equation (see Materials and Methods). Values are the mean ± SEM of data from 3-9 oocytes.

Receptor	EC_{50} (μM)	n_H
WT α4β4	19±4	1.3±0.3
α4H2E β4	21±7	0.9±0.3
α4H2A β4	31±11	1.1±0.4
α4E59A β4	39±10	0.8±0.2
α4H61N β4	19±4	1.2±0.3
α4H104D β4	23±5	1.0±0.2
α4H104A β4	43±10	1.3±0.3
α4H109L β4	17±5	1.4±0.6
α4H162G β4	15±2	1.6±0.3
α4-2 β4	32±6	1.1±0.2
α4 β4C75S	17±3	1.5±0.4
α4 β4H157R	17±3	1.2±0.3
α4 β4D195A	25±3	0.9±0.1
α4 β4H469Y	14±3	1.2±0.2
α4E59A, H162G β4	25±4	1.2±0.2
α4H61N, H162G β4	14±8	1.0±0.7
α4H162G β4H469Y	21±4	1.0±0.1
α4-2 β4C75S (pseudo-WT)	34±12	0.9±0.3
α4-2E59C β4C75S	39±7	1.7±0.5
α4-2H61C β4C75S	23±3	1.2±0.2
α4-2H162C β4C75S	21±3	1.1±0.1
WT α4β2	33±8	1.5±0.4
α4E59Aβ2	42±21	0.8±0.2
α4H162G β2	27±7	1.3±0.3

Molecular Pharmacology Fast Forward. Published on September 27, 2005 as DOI: 10.1124/mol.105.015164
This article has not been copyedited and formatted. The final version may differ from this version.

Table 2. Zinc potentiation of wild-type and mutant neuronal nAChRs. Data is presented as the ratio of potentiation of the mutant receptors to potentiation of wild-type receptors expressed in the same batch of oocytes (mean±SEM, n=3-13). For α4β4, $[Zn^{2+}]$ = 100 μM. For α4β2, $[Zn^{2+}]$ = 50 μM. The overall value for potentiation of wild-type α4β4 was 579±13% of ACh alone (n=48). Significant differences in potentiation, when compared to wild-type α4β4: *p<0.05, **p<0.01, ***p<0.001. The overall value for potentiation of wild-type α4β2 was 241±14% of ACh alone (n=15). Significant differences in potentiation, when compared to wild-type α4β2: †††p<0.001. Fit maximum potentiation, EC_{50} and Hill coefficient (n_H) were determined by fitting the data in Figure 6 to a Hill equation (mean ± SEM, n=4-6).

Receptor	Potentiation (mutant / wt)	Fit Maximum Potentiation (% of ACh)	EC_{50} (μM)	n_H
WT α4β4	1.00	660±53	26±6	1.8±0.5
α4H2E β4	1.08±0.14			
α4H2A β4	0.97±0.09			
α4E59A β4	0.73±0.05***	454±23***	17±2	1.6±0.4
α4H61N β4	0.75±0.10*	444±32***	23±5	1.5±0.4
α4H104D β4	1.21±0.21			
α4H104A β4	0.90±0.11			
α4H109L β4	1.18±0.15			
α4H162G β4	0.45±0.04***	301±19***	18±4	1.5±0.3
α4-2 β4	1.23±0.03*			
α4 β4C75S	0.94±0.06			
α4 β4H157R	0.97±0.13			
α4 β4D195A	0.88±0.05			
α4 β4H469Y	0.82±0.03*	451±16***	21±2	1.4±0.2
α4-2 β4C75S (pseudo-WT)	0.93±0.06			
WT α4β2	1.00			
α4E59Aβ2	0.58±0.13†††			
α4H162G β2	0.38±0.05†††			

Figure 1

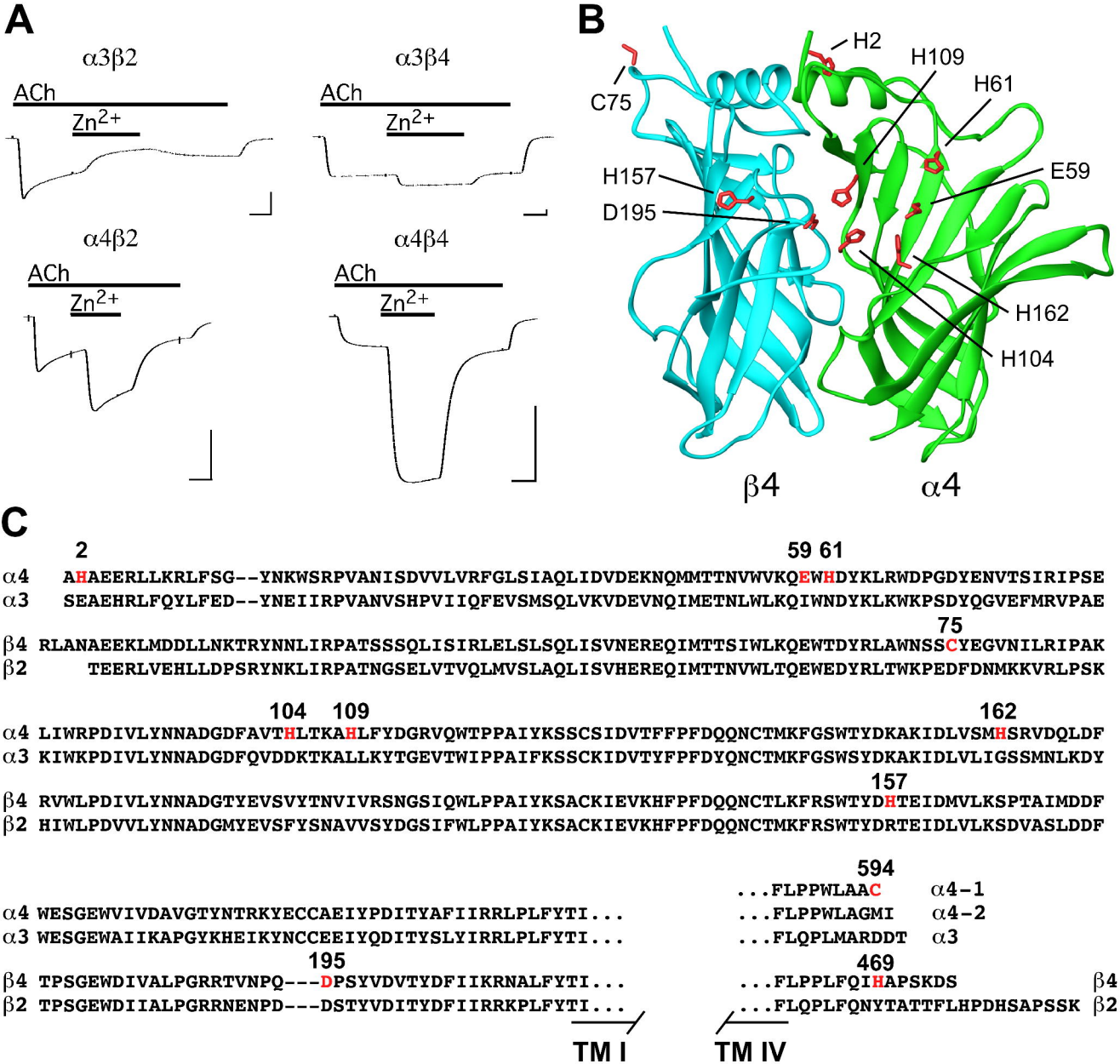
A
α3β2
ACh
Zn2+
α3β4
ACh
Zn2+
α4β2
ACh
Zn2+
α4β4
ACh
Zn2+
B
H2
H109
H61
C75
H157
E59
D195
H162
H104
β4
α4
C
2
59 61
α4 AHAEERLLKRLFSG--YNKWSRPVANISDVVLVRFGLSIAQLIDVDEKNQMMTTNVWVKQEWHDYKLRWDPGDYENVTSIRIPSE
α3 SEAEHRLFQYLFED--YNEIIRPVANVSHPVIIQFEVSMSQLVKVDEVNQIMETNLWLKQIWNDYKLKWKPSDYQGVEFMRVPAE
75
β4 RLANAEEKLMDDLLNKTRYNNLIRPATSSSQLISIRLELSLSQLISVNEREQIMTTSIWLKQEWTDYRLAWNSSCYEGVNILRIPAK
β2 TEERLVEHLLDPSRYNKLIRPATNGSELVTVQLMVSLAQLISVHEREQIMTTNVWLTQEWEDYRLTWKPEDFDNMKKVRLPSK
104 109
162
α4 LIWRPDIVLYNNADGDFAVTHLTKAHLFYDGRVQWTPPAIYKSSCSIDVTFFPFDQQNCTMKFGSWTYDKAKIDLVSMHSRVDQLDF
α3 KIWKPDIVLYNNADGDFQVDDKTKALLKYTGEVTWIPPAIFKSSCKIDVTYFPFDYQNCTMKFGSWSYDKAKIDLVLIGSSMNLKDY
157
β4 RVWLPDIVLYNNADGTYEVSVYTNVIVRSNGSIQWLPPAIYKSACKIEVKHFPFDQQNCTLKFRSWTYDHTEIDMVLKSPTAIMDDF
β2 HIWLPDVVLYNNADGMYEVSFYSNAVVSYDGSIFWLPPAIYKSACKIEVKHFPFDQQNCTMKFRSWTYDRTEIDLVLKSDVASLDDF
594
...FLPPWLAAC α4-1
α4 WESGEWVIVDAVGTYNTRKYECCAEIYPDITYAFIIRRLPLFYTI... ...FLPPWLAGMI α4-2
α3 WESGEWAIIKAPGYKHEIKYNCCEEIYQDITYSLYIRRLPLFYTI... ...FLQPLMARDDT α3
195
469
β4 TPSGEWDIVALPGRRTVNPQ---DPSYVDVTYDFIIKRNALFYTI... ...FLPPLFQIHAPSKDS β4
β2 TPSGEWDIIALPGRRNENPD---DSTYVDITYDFIIRRKPLFYTI... ...FLQPLFQNYTATTFLHPDHSAPSSK β2
TM I
TM IV

Figure 2

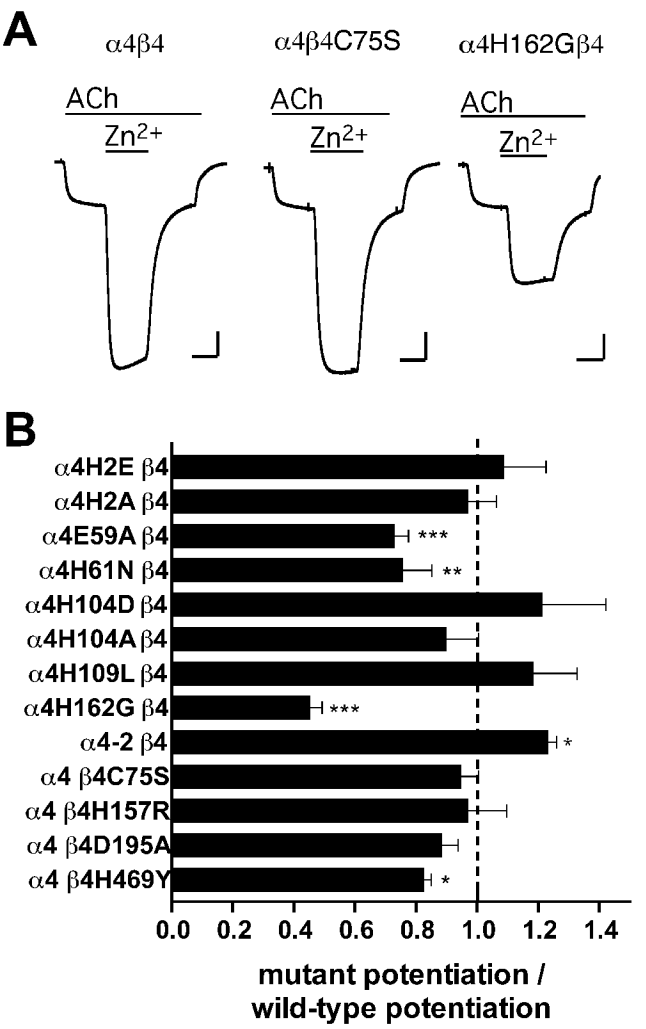
A
α4β4
α4β4C75S
α4H162Gβ4
ACh
Zn2+
B
α4H2E β4
α4H2A β4
α4E59A β4
α4H61N β4
α4H104D β4
α4H104A β4
α4H109L β4
α4H162G β4
α4-2 β4
α4 β4C75S
α4 β4H157R
α4 β4D195A
α4 β4H469Y
***
**
***
*
*
0.0
0.2
0.4
0.6
0.8
1.0
1.2
1.4
mutant potentiation /
wild-type potentiation

Figure 3

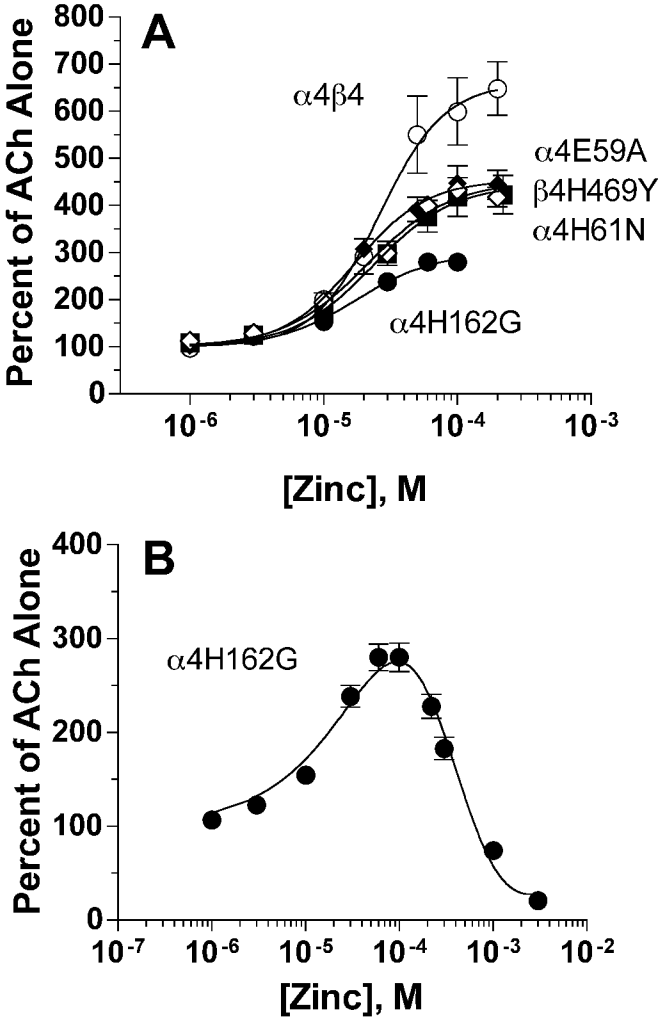
A
Percent of ACh Alone
800
700
600
500
400
300
200
100
0
α4β4
α4E59A
β4H469Y
α4H61N
α4H162G
10-6
10-5
10-4
10-3
[Zinc], M
B
Percent of ACh Alone
400
300
200
100
0
α4H162G
10-7
10-6
10-5
10-4
10-3
10-2
[Zinc], M

Figure 4

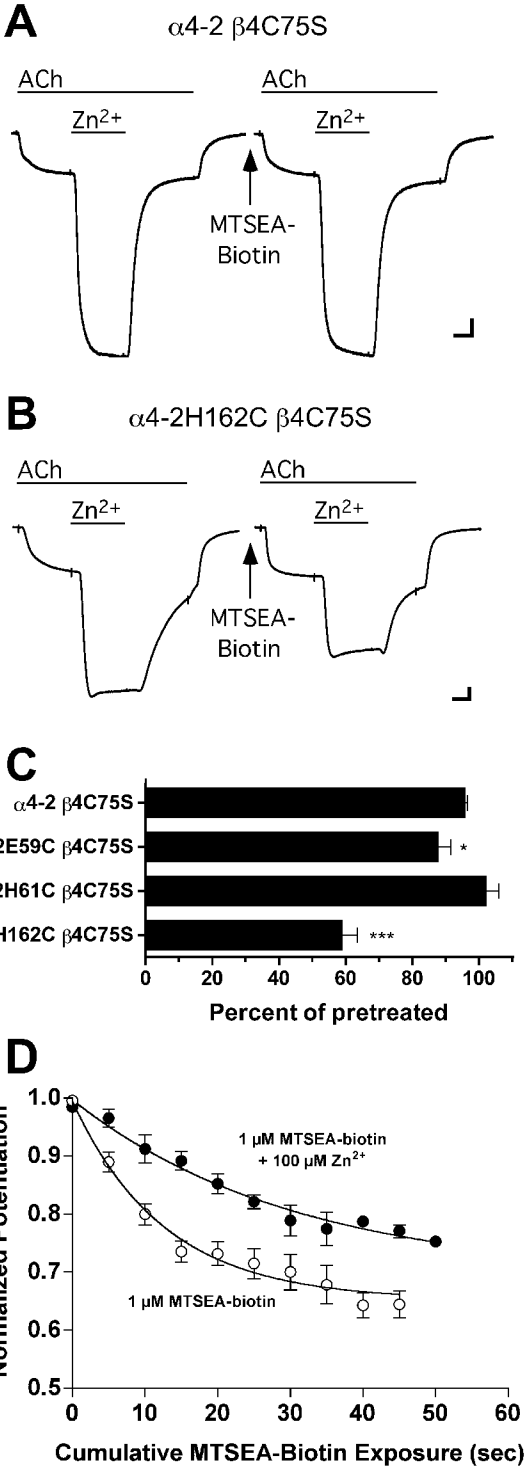
A
α4-2 β4C75S
ACh
ACh
Zn2+
Zn2+
MTSEA-
Biotin
B
α4-2H162C β4C75S
ACh
ACh
Zn2+
Zn2+
MTSEA-
Biotin
C
α4-2 β4C75S
α4-2E59C β4C75S
α4-2H61C β4C75S
α4-2H162C β4C75S
*
***
0
20
40
60
80
100
Percent of pretreated
D
Normalized Potentiation
1.0
0.9
0.8
0.7
0.6
0.5
1 μM MTSEA-biotin
+ 100 μM Zn2+
1 μM MTSEA-biotin
0
10
20
30
40
50
60
Cumulative MTSEA-Biotin Exposure (sec)

Figure 5

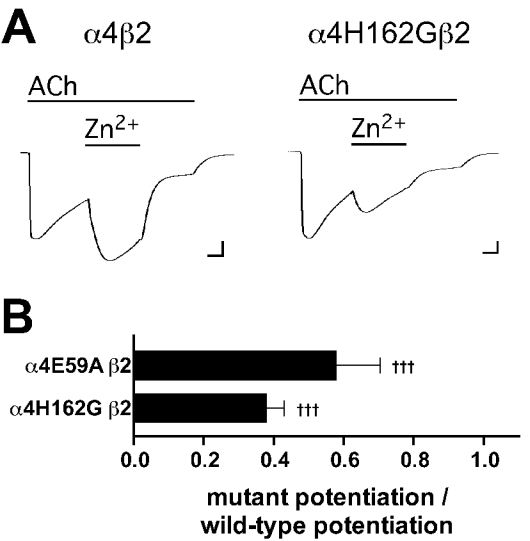
A
α4β2
ACh
Zn2+
α4H162Gβ2
ACh
Zn2+
B
α4E59A β2
α4H162G β2
ttt
ttt
0.0
0.2
0.4
0.6
0.8
1.0
mutant potentiation /
wild-type potentiation

Figure 6